Applied Physics Express **8**, 072502 (2015)
http://dx.doi.org/**10.7567/APEX.8.072502**

Drastic sensitivity enhancement of temperature sensing based on multimodal interference in polymer optical fibers

Goki Numata, Neisei Hayashi, Marie Tabaru, Yosuke Mizuno, and Kentaro Nakamura

Precision and Intelligence Laboratory, Tokyo Institute of Technology, Yokohama 226-8503, Japan

Received April 2, 2015; accepted June 6, 2015; published online June 24, 2015

It has been reported that temperature sensors based on modal interference in perfluorinated graded-index polymer optical fibers show extremely high temperature sensitivity at room temperature. In this work, we confirm that the temperature sensitivity (absolute value) is significantly enhanced when the temperature increases toward ~70 °C, which is close to the glass-transition temperature of the core polymer. When the core diameter is 62.5 μm, the sensitivity at 72 °C at 1300 nm is 202 nm/°C/m, which is approximately 26 times the value obtained at room temperature and >7000 times the highest value previously reported using a silica multimode fiber.

Fiber-optic temperature sensors have been thus far successfully developed by utilizing various physical structures and phenomena, such as fiber Bragg gratings,[1,2] long-period gratings,[3,4] Raman scattering,[5,6] Brillouin scattering,[7–11] and optical interference.[12,13] Among various configurations of interference-based temperature sensors, those based on the interference of multiple guided modes in multimode fibers (MMFs)[14] have been attracting much attention owing to their system simplicity, cost efficiency, and high sensitivity. Since the first demonstration by Mehta et al.,[15] a number of configurations have been implemented (see Table I in Ref. 16). The most commonly used configuration is the so-called "single-mode–multimode–single-mode" (SMS) structure[17–21]—an MMF sandwiched between two single-mode fibers (SMFs).

To date, many researchers have evaluated the performance of SMS-based temperature sensors. Using a 1.8-m-long silica graded-index (GI) MMF, Liu et al.[17] observed a temperature sensitivity of +32.5 pm/°C/m at 1550 nm (corresponding to +27.3 pm/°C/m at 1300 nm, under the simple assumption that the sensitivity is proportional to the optical wavelength). Tripathi et al.[18] experimentally proved that the absolute values, as well as the signs of the temperature sensitivities, are determined by the "critical wavelengths", which depend on the core diameter and/or the dopant of silica MMFs. As SMS-based temperature sensors can also measure strain, the implementation of polymer optical fibers (POFs) as MMFs is a promising method for increasing the maximal measurable strain. Huang et al.[21] developed a large-strain sensor using a 0.16-m-long standard poly(methyl methacrylate) (PMMA) based step-index POF and reported a temperature sensitivity of +581.9 pm/°C/m at 1570 nm (corresponding to +481.8 pm/°C/m at 1300 nm). Nevertheless, PMMA-based POFs suffer from extremely high propagation loss over a wide wavelength range, resulting in an operable POF length inherently limited to <1 m. To overcome this problem, we have recently implemented SMS-based temperature sensors using 1-m-long perfluorinated (PF) GI-POFs,[22] which are the only POFs with relatively low losses of ~250 dB/km even at 1550 nm (or ~50 dB/km at 1300 nm). When the core diameter was 62.5 μm, the obtained temperature sensitivity at room temperature at 1300 nm was as high as +49.8 nm/°C/m.[23] This corresponds to the highest yet reported absolute value, over 1800 times and 100 times higher than those measured in a silica GI-MMF[17] and a PMMA-based POF,[21] respectively. However, the sensing performance of these sensors was evaluated only at room temperature, and no reports have been provided at high temperature, close to the glass-transition temperature.

In this work, we investigate the performance of temperature sensors composed of 1-m-long PFGI-POFs with three different core diameters (50, 62.5, and 120 μm) in a wide temperature range from room temperature to high temperatures near the glass-transition temperature. When the core diameter was 62.5 μm, the temperature sensitivity (absolute value) increased with increasing temperature, reaching +202 nm/°C/m at ~72 °C, which is ~7400 times higher than that measured at room temperature. This behavior is unique to POFs with relatively low glass-transition temperature, which was confirmed by showing that the temperature sensitivity of a silica MMF-based sensor does not change with increasing temperature to 130 °C. In general, the glass-transition temperature of polymers can be arbitrarily adjusted; thus, we expect that in the future, by exploiting this unique property of POF sensors, ultra-high temperature sensing will be feasible not only at ~70 °C, but at arbitrary temperatures.

The SMS structure generally comprises an MMF sandwiched by identical SMFs. At the first SMF-to-MMF interface, light is guided from the lead-in SMF into the MMF. The spot-size difference between the fundamental (or 0-th) modes in the SMF and the MMF excites a few lower modes in the MMF, which propagate along the MMF with their respective propagation constants. Then, at the second MMF-to-SMF interface, the net field coupled to the lead-out SMF is determined by the relative phase differences between the multiple modes guided in the MMF. Supposing that the MMF and SMFs are axially aligned, only the axially symmetric modes are excited in the MMF. A detailed calculation[20] gives an expression of the optical power in the lead-out SMF as

$$P_{\mathrm{out}} = |a_0^2 + a_1^2 \exp i(\beta_0 - \beta_1)L + a_2^2 \exp i(\beta_0 - \beta_2)L + \cdots|^2, \quad (1)$$

where a_i is the field amplitude of the i-th mode at the first SMF-to-MMF interface, β_i is the propagation constant of the i-th mode, and L is the MMF length. This equation shows that the optical power in the lead-out SMF is affected by physical changes caused by strain and temperature, as they have non-negligible influence on the propagation constants and the MMF length. These changes can be quantitatively evaluated by measuring the shift of spectral dips (or peaks).

The temperature sensitivity is often expressed using units of "pm/°C/cm", where the value expressed with "cm" is the length of the heated section. When the whole length of the MMF is heated, it corresponds to the MMF length itself. This

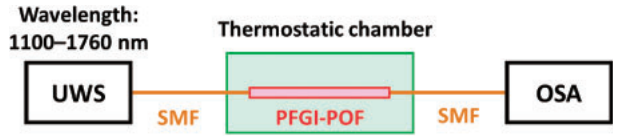

Fig. 1. Schematic of the experimental setup. OSA: optical spectrum analyzer; PFGI-POF: perfluorinated graded-index polymer optical fiber; SMF: single-mode fiber; UWS: ultra-wideband source.

can be explained as follows: for simplicity, suppose the interference of the lights only of the fundamental and first-order higher modes propagating along the MMF. If the MMF length is the same, a longer heated section leads to their longer optical-path difference (due to thermal expansion), resulting in a larger temperature-dependence coefficient of the dip wavelength. Similarly, even when the MMF length is reduced, if the length of the heated section remains the same, the induced optical-path difference (and thus the temperature-dependence coefficient) is unchanged. Therefore, when the full length of the MMF is heated, the use of the unit "pm/°C/cm" (or "nm/°C/m", in the case of PFGI-POFs) is valid.

The MMFs used in the experiment were PFGI-POFs with three different core diameters (50, 62.5, and 120 μm), and their core and cladding layers were composed of doped and undoped poly(perfluorobutenylvinyl ether), respectively. The lengths of the three PFGI-POFs were all set to 1 m, similarly to those used in Ref. 23, for an easy comparison of their sensing characteristics. The refractive indices at the center of the core and in the cladding layer were approximately 1.35 and 1.34, respectively, regardless of the optical wavelength.[24] Outside the cladding layer, an overcladding layer (diameter: 500 μm) composed of polycarbonate was coated to suppress microbending loss and to improve the load-bearing capability.

Figure 1 depicts an experimental setup for characterizing the PFGI-POF-based temperature sensors in a wide temperature range. Both ends of the PFGI-POF were butt-coupled to silica SMFs via "SC/PC-FC/PC" adaptors,[25] and the whole length of the PFGI-POF was placed in a thermostatic chamber to control the ambient temperature (the heated adaptors were confirmed to have no quantifiable influence on the experimental results). Because spectral measurements with the widest possible span were preferable for this experiment, we employed an ultra-wideband source (Santec UWS-1000) that emits super-continuum light with an output spectrum from 1100 to 1760 nm (pumped at 1550 nm), instead of the wavelength-tunable laser used in previous reports.[23,26] The spectral power density of the source was higher than −30 dBm/nm over the full range; this value is much larger than that of a standard white-light source, which cannot be used in this case because of the high propagation loss of the PFGI-POF. The ultra-wideband source output was injected into the PFGI-POF, and the transmission spectrum was measured using an optical spectrum analyzer (OSA). The room temperature was 20 °C.

The measured optical spectra of the PFGI-POF with 50 μm core diameter before and after transmission at room temperature are shown in Fig. 2. Before transmission, a relatively flat spectrum ranging from 1100 to 1760 nm was observed. The peak at 1550 nm corresponds to the pump frequency of the super-continuum generation. After transmission, both a relatively uniform ∼10–20 dB loss and a wavelength-dependent loss were observed in the spectrum, resulting in several characteristic dips and peaks. These dips and peaks originate from modal interference and their wavelengths are dependent on the ambient temperature of the POF.

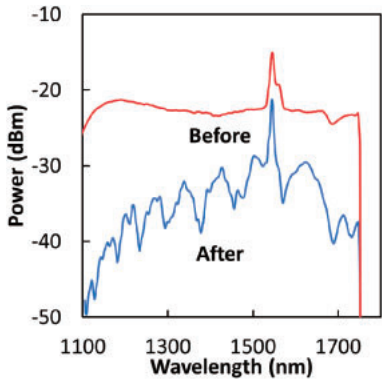

Fig. 2. Measured optical spectra before and after transmission through the PFGI-POF.

We then investigated the wide-range temperature dependence of the wavelengths of some relatively clear spectral dips in the spectrum of the PFGI-POF with 50 μm core diameter [Fig. 3(a)]. The measured data are discontinuously plotted because of two reasons: (1) a measurement at one fixed temperature required ∼10 min because of the time needed for the temperature to stabilize. Therefore, the measurements were performed separately in each 10 °C interval (i.e., 20–30 °C, 30–40 °C), and the corresponding data were merged later (some peaks appeared or disappeared with time owing to polarization fluctuations;[17] this instability could be mitigated by employing polarization diversity or polarization scrambling). (2) When the dips shifted close to the 1550 nm pump peak, they were buried in the spectral floor (this problem could be resolved by the use of a properly designed optical filter at 1550 nm). As shown in Fig. 3(a), with increasing temperature, the wavelengths of all the dips decreased. The dependence coefficient at room temperature at 1300 nm was approximately −5.3 nm/°C/m (calculated by interpolation/extrapolation), which moderately agrees with the previously reported value (−4.7 nm/°C/m).[23] In this wavelength range, the absolute values of the coefficients at shorter wavelengths were slightly smaller than those at longer wavelengths, which indicates that the critical wavelength[18] is longer than ∼1700 nm. In the temperature range from 20 to ∼50 °C, the dependence coefficient of all dips remained almost constant; however, over ∼50 °C, their absolute values gradually increased. The coefficient at 67 °C at 1300 nm reached −85 nm/°C/m, which was ∼16 times the value at room temperature. Over ∼67 °C, the spectral change was so drastic that correct measurements were no longer possible.

Subsequently, we confirmed that this peculiar behavior is a unique characteristic of POFs by performing the same measurement using a silica GI-MMF with the same core diameter (50 μm). Figure 3(b) shows the dip wavelengths measured as functions of temperature in the range from 20 to 130 °C. The dependence coefficient at room temperature at 1300 nm (−2.2 nm/°C/m) was similar to that at ∼130 °C (−2.3 nm/°C/m), which indicates that the gradual temperature-dependent change in the coefficients (in this temperature range) is unique to POFs. This behavior, similar to the nonlinear tem-

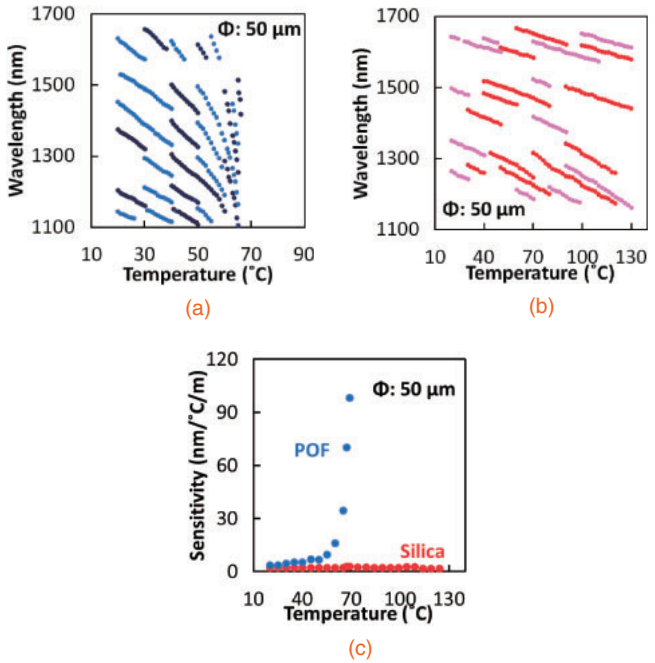

Fig. 3. Temperature dependence of the dip wavelength in a wide temperature range for (a) the PFGI-POF and (b) the silica GI-MMF with 50 μm core diameter. The different colors represent different dips. (c) Temperature sensitivity (absolute value of the temperature-dependence coefficients) at 1300 nm in the PFGI-POF and the silica GI-MMF plotted as functions of temperature.

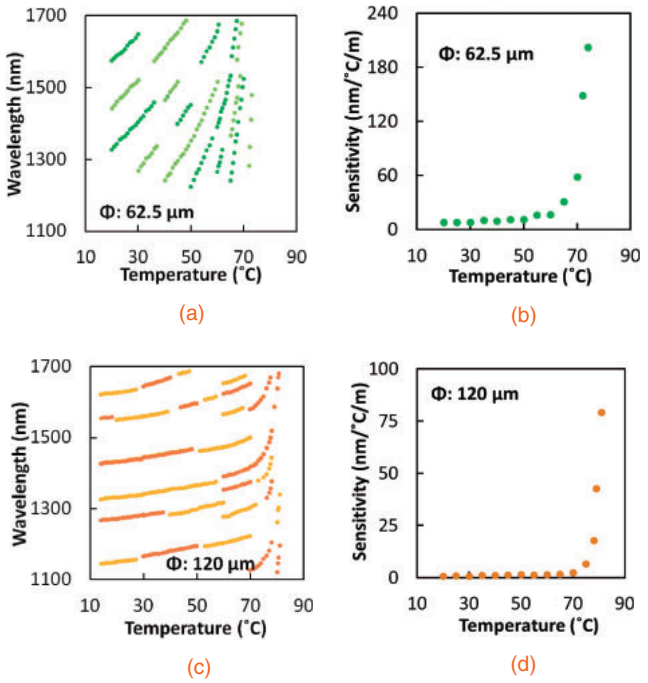

Fig. 4. Temperature dependence of (a) the dip wavelengths and (b) the coefficient of the PFGI-POF with 62.5 μm core diameter and of (c) the dip wavelength and (d) the coefficient of the PFGI-POFs with 120 μm core diameter.

perature dependence of the Brillouin frequency shift in POFs,[27] seems to result from the partial phase transition of the polymer material. The temperature of ~67 °C, at which the largest coefficient (absolute value) was obtained for the PFGI-POF, probably corresponds to the glass-transition temperature of poly(perfluorobutenylvinyl ether) (~108 °C; note that the phase transition, which has some influence on the thermal expansion coefficient and each modal index, generally occurs at a temperature of approximately 50 °C in polymers[28] and that the starting temperature of the phase transition is lower than the glass-transition temperature by several tens of degrees). Figure 3(c) shows the temperature sensitivities, i.e., the absolute values of the temperature-dependence coefficients of the dip wavelengths, at 1300 nm for the PFGI-POF and the silica GI-MMF, plotted as functions of temperature. It is clear that the temperature sensitivity of the PFGI-POF increases abruptly at 67 °C, while that of the silica GI-MMF remains almost constant. Measurements using the silica GI-MMF up to its glass-transition temperature (~1000 °C) would provide even more reliable information.

We also performed the same measurements using the PFGI-POFs with 62.5 and 120 μm core diameters [Figs. 4(a)–4(d)]. In both cases, the dip wavelengths increased with increasing temperature. The difference in the absolute value and the sign has been previously reported[23] and explained by the structural influence on the critical wavelengths[18] (which are shorter than 1100 nm for the 62.5-μm-core PFGI-POF and longer than 1700 nm for the 120-μm-core PFGI-POF). The coefficients at room temperature at 1300 nm were +7.7 nm/°C/m for the 62.5-μm-core PFGI-POF and +1.1 nm/°C/m for the 120-μm-core PFGI-POF. The difference between these values and those previously reported[23] is probably caused by the manually prepared end-surfaces and lot-to-lot non-uniformity, leading to the different excited modes. The maximal values obtained at high temperature at 1300 nm were +202 nm/°C/m for the 62.5-μm-core PFGI-POF and +85.6 nm/°C/m for the 120-μm-core PFGI-POF, which are ~26 and ~78 times larger, respectively, than those measured at room temperature. The temperature sensitivity of +202 nm/°C/m at 1300 nm, obtained at ~72 °C using the 62.5-μm-core PFGI-POF, is well over 7000 times larger than the highest value previously reported for a silica GI-MMF;[17] to the best of our knowledge, this is the highest value ever reported in modal-interference-based temperature sensors. The temperatures at which the largest temperature sensitivities (absolute values of the temperature-dependence coefficients) were experimentally obtained were ~69, ~72, and ~82 °C for the PFGI-POFs with 50, 62.5, and 120 μm core diameters, respectively, suggesting a positive correlation between the highest operable temperature and the core diameter of the POF. It would be worthwhile to clarify this point, although PFGI-POFs with other core diameters are not commercially available at present.

In conclusion, we investigated the performance of SMS-based temperature sensors comprising 1-m-long PFGI-POFs with 50, 62.5, and 120 μm core diameters in a wide temperature range. When the core diameter was 62.5 μm, the temperature sensitivity, i.e., the temperature-dependence coefficients of the spectral dips, increased with increasing temperature, reaching +202 nm/°C/m at ~72 °C at 1300 nm; this value is over 7000 times higher than that obtained at room temperature. Over ~72 °C, a correct measurement was difficult owing to spectral instability. We verified that this behavior is unique to POFs with relatively low glass-transition temperature by demonstrating that the temperature

sensitivity of a silica-MMF-based sensor exhibits almost no change with increasing temperature up to 130 °C. We also showed that the highest operable temperature might be correlated to the core diameter of the PFGI-POFs. Furthermore, considering that the phase-transition temperature of polymers can be controlled by adding plasticizers and by copolymerizing/blending different materials,[29] we expect that such ultra-high temperature sensitivity will be achievable not only near 70–80 °C but also at arbitrary temperatures, opening the way for more useful and practical applications.

Acknowledgments We are indebted to Professors Fumio Koyama and Hiroyuki Uenohara (Precision and Intelligence Laboratory, Tokyo Institute of Technology) for permitting us to use their ultra-wideband light source. This work was partially supported by Grants-in-Aid for Young Scientists (A) (No. 25709032) and for Challenging Exploratory Research (No. 26630180) from the Japan Society for the Promotion of Science (JSPS) and by research grants from the Iwatani Naoji Foundation, the SCAT Foundation, and the Konica Minolta Science and Technology Foundation. N.H. acknowledges a Grant-in-Aid for JSPS Fellows (No. 25007652).

1) J. Jung, H. Nam, B. Lee, J. O. Byun, and N. S. Kim, Appl. Opt. **38**, 2752 (1999).
2) B.-O. Guan, H.-Y. Tam, X.-M. Tao, and X.-Y. Dong, IEEE Photonics Technol. Lett. **12**, 675 (2000).
3) V. Bhatia and A. M. Vangsarkar, Opt. Lett. **21**, 692 (1996).
4) Y.-P. Wang, L. Xiao, D. N. Wang, and W. Jin, Opt. Lett. **31**, 3414 (2006).
5) M. A. Farahani and T. Gogolla, J. Lightwave Technol. **17**, 1379 (1999).
6) M. N. Alahbabi, Y. T. Cho, and T. P. Newson, Opt. Lett. **30**, 1276 (2005).
7) T. Horiguchi and M. Tateda, J. Lightwave Technol. **7**, 1170 (1989).
8) T. Kurashima, T. Horiguchi, H. Izumita, S. Furukawa, and Y. Koyamada, IEICE Trans. Commun. **E76-B**, 382 (1993).
9) D. Garus, K. Krebber, F. Schliep, and T. Gogolla, Opt. Lett. **21**, 1402 (1996).
10) K. Hotate and T. Hasegawa, IEICE Trans. Electron. **E83-C**, 405 (2000).
11) Y. Mizuno, W. Zou, Z. He, and K. Hotate, Opt. Express **16**, 12148 (2008).
12) Y. J. Rao, D. A. Jackson, L. Zhang, and I. Bennion, Opt. Lett. **21**, 1556 (1996).
13) Y. Chen and H. F. Taylor, Opt. Lett. **27**, 903 (2002).
14) J. Zhang, Y. Zhang, W. Sun, and L. Yuan, Meas. Sci. Technol. **20**, 065206 (2009).
15) A. Mehta, W. Mohammed, and E. G. Johnson, IEEE Photonics Technol. Lett. **15**, 1129 (2003).
16) O. Frazão, S. O. Silva, J. Viegas, L. A. Ferreira, F. M. Araújo, and J. L. Santos, Appl. Opt. **50**, E184 (2011).
17) Y. Liu and L. Wei, Appl. Opt. **46**, 2516 (2007).
18) S. M. Tripathi, A. Kumar, R. K. Varshney, Y. B. P. Kumar, E. Marin, and J. P. Meunier, J. Lightwave Technol. **27**, 2348 (2009).
19) S. M. Tripathi, A. Kumar, R. K. Varshney, Y. B. P. Kumar, E. Marin, and J. P. Meunier, J. Lightwave Technol. **28**, 3535 (2010).
20) A. Kumar, R. K. Varshney, S. C. Antony, and P. Sharma, Opt. Commun. **219**, 215 (2003).
21) J. Huang, X. Lan, H. Wang, L. Yuan, T. Wei, Z. Gao, and H. Xiao, Opt. Lett. **37**, 4308 (2012).
22) Y. Koike and M. Asai, NPG Asia Mater. **1**, 22 (2009).
23) G. Numata, N. Hayashi, M. Tabaru, Y. Mizuno, and K. Nakamura, IEEE Photonics J. **6**, 6802306 (2014).
24) T. Ishigure, Y. Koike, and J. W. Fleming, J. Lightwave Technol. **18**, 178 (2000).
25) Y. Mizuno and K. Nakamura, Appl. Phys. Lett. **97**, 021103 (2010).
26) G. Numata, N. Hayashi, M. Tabaru, Y. Mizuno, and K. Nakamura, IEICE Electron. Express **12**, 20141173 (2015).
27) K. Minakawa, N. Hayashi, Y. Shinohara, M. Tahara, H. Hosoda, Y. Mizuno, and K. Nakamura, Jpn. J. Appl. Phys. **53**, 042502 (2014).
28) M. Naritomi, H. Murofushi, and N. Nakashima, Bull. Chem. Soc. Jpn. **77**, 2121 (2004).
29) K. Koike, H. Teng, Y. Koike, and Y. Okamoto, Polym. Adv. Technol. **25**, 204 (2014).